WELDING OF TITANIUM AND ALUMINUM ALLOYS USING OSCILLATING ELECTRON BEAM AND NIOBIUM FILLER

Darina Kaisheva[1,2], Borislav Stoyanov[3], Vladimir Dunchev[3], Georgi Kotlarski[1], Maria Ormanova[1], Stefan Valkov[1,3]

[1]Academician Emil Djakov Institute of Electronics, Bulgarian Academy of Sciences, 72 Tzarigradsko Chausse Blvd, 1784 Sofia, Bulgaria
[2] South-West University „Neofit Rilski“, 66 Ivan Michailov Str., 2700 Blagoevgrad, Bulgaria
[3] Technical University of Gabrovo, 4 H. Dimitar Str., 5300 Gabrovo, Bulgaria

Abstract

Titanium, aluminum and their alloys are increasingly used in a number of industries. Due to their very different thermo-physical parameters, obtaining a strong joint between them is rather difficult. Electron beam technology has been successfully applied to weld Ti/Ti alloys to Al/Al alloys. The aim of the present work is to investigate the influence of specific technological conditions, including the use of niobium filler, on the structure and mechanical properties of an electron beam welded joint of titanium alloy Ti6Al4V and aluminum alloy Al6082-T6. EBW was carried out at following technological conditions: accelerating voltage U=60 kV; beam current I_b=25 mA; welding speed v=10 mm/s; section length of the along linear electron beam oscillation l=6 mm; oscillation frequency f=200 Hz. The Nb filler was deposited via magnetron sputtering method. The phase composition of the weld was obtained using X-ray diffraction (XRD). Scanning electron microscopy (SEM) and energy-dispersive X-ray spectroscopy (EDX) analysis were used to investigate the structure of the welded joint. The Vickers microhardness in a line perpendicular to the weld seam in the middle depth was measured. The formation of intermetallic phases Ti_3Al, TiAl, $TiAl_3$ and $NbAl_3$ was established, also proven by the measured high hardness, reaching 627 $HV_{0.5}$.

Keywords: electron beam welding, dissimilar materials, aluminum alloy, titanium alloy, oscillating electron beam, niobium filler.

INTRODUCTION

Titanium, aluminum and their alloys are increasingly used in a number of industries, most notably aircraft and automotive [1-4]. They are preferred because of their low density, which reduces energy costs, while at the same time exhibiting high strength. These materials also have high corrosion resistance, even at high temperatures. Besides that, another advantage of them is their high plasticity, especially of aluminum, which helps to process them easily.

However, due to their very different thermo-physical properties [5], obtaining a strong joint between titanium and aluminum is rather difficult. Various technologies have been used to weld titanium and aluminum alloys, such as diffusion welding [6], explosive welding [7], friction stir welding [8-10], laser welding [11,12]. Electron-beam welding (EBW) is one of the most common techniques used for welding Ti and Al due to a number of advantages. During EBW a deep and narrow seam is obtained with minimal deformations and residual stresses. In this method, no additives are used, moreover, the process takes place in vacuum, which results in the absence of impurities in the seam. Electron beams have been successfully applied as heat sources to weld Ti/Ti alloys to Al/Al alloys [13,14]. In our previous work [14], we have investigated the influence of the offset of the electron beam from the gap between Ti6Al4V plates and Al6082-T6 plates on the structure and mechanical properties of the resultant weld seam.

A problem in welding titanium and aluminum is the formation of intermetallic compounds, which are very brittle and hard and lead to a reduction in the ductility and strength of the joint. A way to control the intermetallic phase growth process is the application of an electron beam oscillation [15]. This way, the duration of the molten phase of the weld seam and the solidification time are controlled more precisely. Another way to affect the formation of the intermetallic phases is the use of an insert of a third material as a filler [16].

The aim of the present work is to investigate the influence of specific technological conditions, including the use of niobium filler, on the structure and mechanical properties of an electron beam welded joint of titanium alloy Ti6Al4V and aluminum alloy Al6082-T6.

MATERIALS AND METHODS

In the experiments a Ti6Al4V (Ti64) plate and an Al6082-T6 plate with dimensions of 100x50x8 mm were used. The chemical composition of the welded alloys is shown in Table 1.

Table 1. *Chemical composition of the Ti6Al4V and Al6082-T6 alloys.*

Al 6082-T6		Ti6Al4V	
Element	wt, %	Element	wt, %
Si	0.7-1.3	Al	5.5-6.5
Mg	0.6-1.2	V	3.5-4.5
Mn	0.4-1.0	Fe	0.25
Fe	0.5	Ti	Bal.
Cr	0.1		
Al	Bal.		

A layer of pure Nb was previously deposited on the transverse surfaces of both plates using direct current magnetron sputtering. The two coated surfaces were conjoined mechanically and electron-beam welded. The process of forming the coatings involved two stages: cathodic cleaning and deposition. Cathodic cleaning was performed under the following conditions: working pressure p_{cc}=6.10^{-5} mbar; discharge voltage U_{cc}=750 V; discharge current I_{cc}=0.1 A and cleaning time t_{cc}=10 min. The deposition of the layers of pure niobium was performed under the following conditions: working pressure p_d=8.10^{-4} mbar; discharge voltage U_d=410 V; discharge current I_d=1 A and deposition time t_d=150 min.

EBW was carried out on the Evobeam Cube 400 welding unit manufactured by Evobeam GmbH, using the following technological conditions: accelerating voltage U=60 kV; beam current I_b=25 mA; welding speed v=10 mm/s; section length of the along linear electron beam oscillation l=6 mm; oscillation frequency f=200 Hz. The scheme of the experiment is shown in Fig. 1.

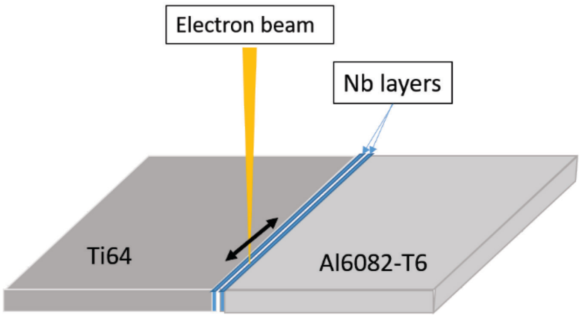

Fig. 1. *Schematic of the process of EBW of Ti64 and Al6082-T6 with oscillating beam and Nb filler.*

X-ray diffraction experiments (XRD) were performed to determine the phase composition of the weld seam. The experiments were realized using Cu Kα characteristic radiation with λ=1.54060 Å on diffractometer "Bruker D8 Advance", Brucker Corp. The measurement method used a symmetrical Bragg-Brentano mode from 30 to 70 degrees at 2θ scale with a step of 0.05° and a counting time of 1s per step.

Scanning electron microscopy (SEM) was used to study the microstructure of the investigated sample. The SEM images were obtained via microscope "LYRA I XMU", Tescan Orsay Holding, using back scattered electrons.

The Vickers microhardness was measured on a semi-automatic microhardness tester "ZWICK/Indentec - ZHVμ-S", ZwickRoell GmbH & Co. KG, in the middle of the weld seam along the line perpendicular to the welding direction. A loading force of 0.5 N was applied all experimental points.

RESULTS AND DISCUSSION

The X-ray diffraction patterns of the weld are presented in Fig. 2. Peaks corresponding to the pure metals Ti, Al and Nb, as well as intermetallic compounds between Ti/Al and Nb/Al are visible.

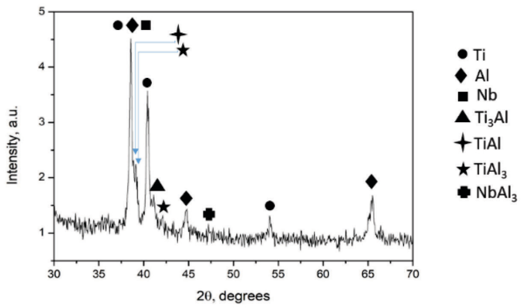

Fig. 2. *X-ray diffraction patterns of the welded joint.*

According to the International Centre for Diffraction Data (ICDD) database, peaks corresponding to Ti_3Al, TiAl, $TiAl_3$ and $NbAl_3$ are found.

SEM images of the weld seam and different sections of it with different magnification are shown on Fig. 3. From Fig. 3 (a), it can be seen that in the welding process, full penetration was not achieved and the height of the weld seam is half the thickness of the plates. The welding seam has the characteristic EBW shape of a "keyhole" with molten metal pouring over the titanium plate. In the fusion zone (FZ) of the weld, two subzones are clearly distinguished - on the side of the aluminum alloy, marked in Fig. 3(c) as FZ-A and on the side of the titanium alloy indicated in Fig. 3(c) as FZ-B. The presence of two subzones in the FZ is indicative of insufficient homogenization of the molten materials. This is evidenced by the formation of non-uniform structures, especially in FZ-A, as seen in Fig. 3(c). Micro-cracks are visible in the middle of the weld along its height in the zone between the titanium rich and the

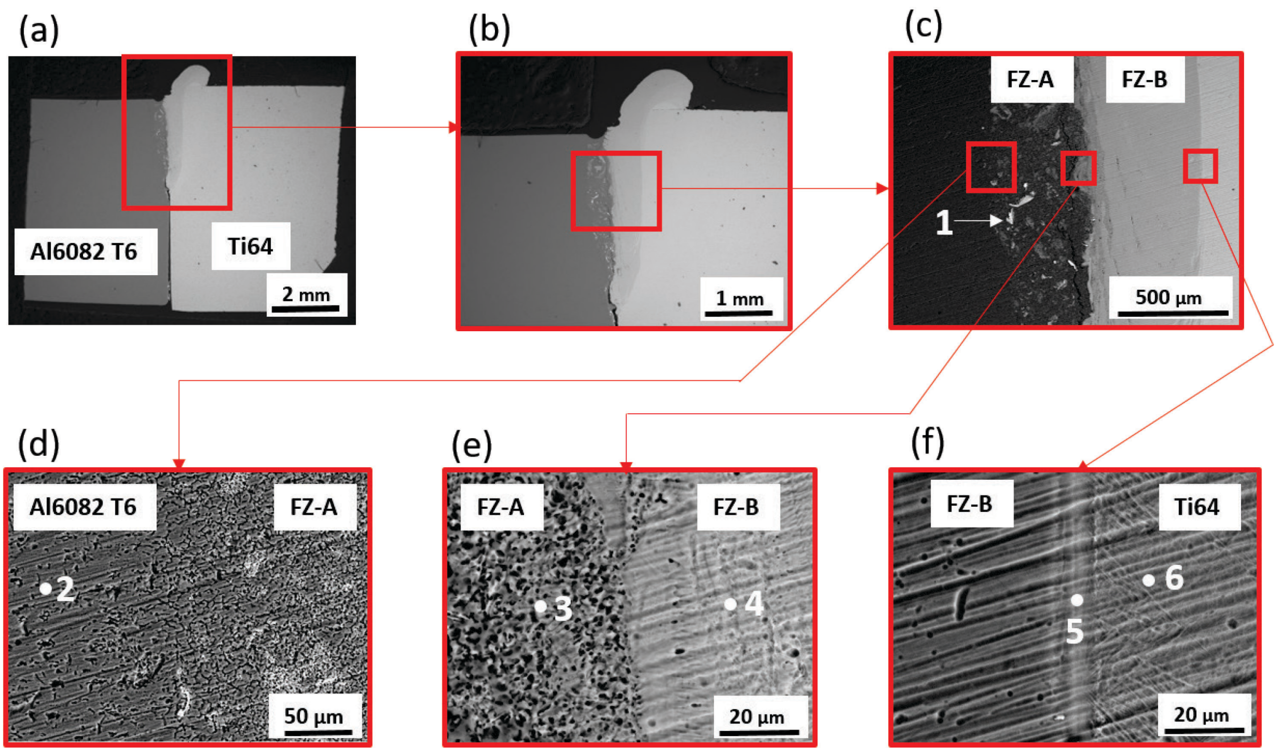

Fig. 3. *Cross-sectional SEM images of the welded joint: (a) both jointed plates; (b) weld seam as a whole; (c) part of the weld seam; (d) interface Al6082-T6 / fusion zone-A; (e) interface fusion zone-A / fusion zone-B; (f) interface fusion zone-B / Ti64.*

aluminum rich areas of the weld seam (Fig. 3(b)). These cracks are most probably the result of the poor mixture between the Ti64 alloy and the Al alloy. The different thermophysical properties of the two formed zones results in the different behavior of the formed compounds in them. Due to this during the solidification stage defects in the structure of the weld seam form such as hot cracks. Under the selected technological conditions, the life of the molten pool was not sufficient enough to form a homogeneous weld seam with an equilibrium structure, regardless of the fact that the oscillation of the electron beam increases the time of the existing liquid phase. Martensitic lamellae are seen in Fig. 3 (f) at the boundary between the heat affected zone of the titanium alloy and FZ-B. The appearance of martensite is due to the high cooling rates characteristic of EBW. The presence of martensite is also evidenced by the measured microhardness shown below. From the performed EDX analysis, it is clear the formation of intermetallic phases, fully corresponding to the XRD analysis shown above. The results of the EDX analysis into and around the fusion zone in points marked in Fig. 3 (c)-(f), are shown in Table 2. EDX analysis proves the formation of the intermetallic phases Ti_3Al, TiAl, $TiAl_3$ and $NbAl_3$ according to the binary phase diagrams Ti/Al and Nb/Al. The Ti-rich phases are formed closer to the titanium alloy in the FZ-A subzone, and the Al- rich phases are seen in the subzone FZ-B, located close to the aluminum alloy.

Table 2. *Chemical composition and assumptions of the potential phases in the weld.*

	Al, at.%	Ti, at.%	V, at.%	Nb, at.%	Potential phase
point 1	69.56	1.69	0.27	28.48	$NbAl_3$
point 2	99.59	0.10	0.14	0.14	Al
point 3	74.00	24.28	0.78	0.94	$TiAl_3$
point 4	53.71	43.60	1.21	1.48	TiAl
point 5	20.02	77.71	1.59	0.69	Ti_3Al
point 6	10.65	87.16	1.68	0.51	Ti64

The distribution of the measured Vickers microhardness is presented in Fig. 4.

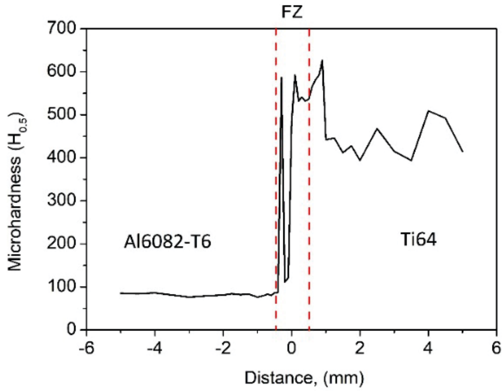

Fig. 4. *Microhardness distribution across the weld.*

The hardness of the aluminum alloy has a value of 80 $HV_{0.5}$. In the fusion zone, the hardness increases sharply and fluctuates between 532 $HV_{0.5}$ and 592 $HV_{0.5}$. In the heat affected zone of the Ti64 plate, the hardness reaches a maximum value of 627 $HV_{0.5}$. This increase in hardness supports the above statement that a phase transformation has taken place in the titanium alloy and a martensite structure has formed. The titanium alloy has a microhardness of about 400 $HV_{0.5}$, characteristic of Ti64.

CONCLUSION

The following conclusions can be drawn from the conducted research:

- The applied technological conditions of EBW were insufficient to achieve full penetration of the welded metallic plates;
- During the electron beam welding process defects such as hot cracks formed in the structure of the weld seam due to the substantially different thermophysical properties of Ti and Al, and their respective phases;
- The high concentration of intermetallic phases results in a substantial increase of the microhardness of the weld seam. This leads to a weakening of the formed weld and to an increase of its brittleness;
- The application of a Nb interlayer between the two welded surfaces and the use of an oscillating electron beam both led to an improved mixture of the Ti and Al alloys, and

to an increase of the controllability of the welding process. However, it is clear that under the selected technological conditions the homogenization of the melt is not sufficient despite the application of beam oscillation and the use of filler;

- Regardless of the better controllability of the process the high presence of defects and the high hardness of the weld seam lead to a worsening of the mechanical properties of the weld and substantially limit its applicability.

In future research, it is necessary to look for more suitable technological conditions of the EBW process of Ti64 and Al6082-T6 in order to obtain joints with improved mechanical properties.

ACKNOWLEDGEMENTS

This work was supported by Bulgarian National Scientific Found under Grant No KP06-N47/6.

REFERENCE

[1] Stojanovic, B., Bukvic, M., & Epler, I. (2018). Application of aluminum and aluminum alloys in engineering. *Applied engineering letters: Journal of Engineering and Applied Sciences*. Vol.3, No.2, 52-62

[2] Schauerte, Oliver. "Titanium in automotive production." *Advanced engineering materials* 5.6 (2003): 411-418.

[3] Williams, James C., and Rodney R. Boyer. "Opportunities and issues in the application of titanium alloys for aerospace components." *Metals* 10.6 (2020): 705.

[4] Anil Kumar, V., et al. "Recent advances in processing of titanium alloys and titanium aluminides for space applications: A review." *Journal of Materials Research* 36 (2021): 689-716.

[5] Cverna, F. (Ed.). (2002). *ASM ready reference: thermal properties of metals*. ASM International.

[6] Enjyo, T., Ikeuchi, K., Kanai, M., & Maruyama, T. (1977). Diffusion welding of aluminum to titanium. *Transactions of JWRI*, *6*(1), 123-130.

[7] Bi, Z. X., Li, X. J., Zhang, T. Z., Wang, Q., Rong, K., Dai, X. D., & Wu, Y. (2022). Microstructure and characterization of Ti–Al explosive welding composite plate. *The International Journal of Advanced Manufacturing Technology*, *123*(5), 1825-1833.

[8] Wu, A., Song, Z., Nakata, K., Liao, J., & Zhou, L. (2015). Interface and properties of the friction stir welded joints of titanium alloy Ti6Al4V with aluminum alloy 6061. *Materials & Design*, *71*, 85-92.

[9] Dressler, U., Biallas, G., & Mercado, U. A. (2009). Friction stir welding of titanium alloy TiAl6V4 to aluminium alloy AA2024-T3. *Materials Science and Engineering: A*, *526*(1-2), 113-117.

[10] Sundar, A. S., Vardhan, T. V., & Kumar, A. (2022). Microstructural characterization of aluminium-titanium friction stir welds. *Materials Today: Proceedings*, *62*, 5845-5849.

[11] Raja Kumar, M., Jouvard, J. M., Tomashchuk, I., & Sallamand, P. (2020). Vapor plume and melted zone behavior during dissimilar laser welding of titanium to aluminum alloy. *Proceedings of the Institution of Mechanical Engineers, Part L: Journal of Materials: Design and Applications*, *234*(5), 681-696.

[12] Vaidya, W. V., Horstmann, M., Ventzke, V., Petrovski, B., Koçak, M., Kocik, R., & Tempus, G. (2010). Improving interfacial properties of a laser beam welded dissimilar joint of aluminium AA6056 and titanium Ti6Al4V for aeronautical applications. *Journal of materials science*, *45*, 6242-6254.

[13] Havlík, P., Kouřil, J., Foret, R., Dlouhy, I., Enzinger, N., & Wiednig, C. (2017). Evaluation of weldability of titanium alloy Ti-6Al-4V and aluminum alloy 6061 produced by electron beam welding. In *Materials Science Forum* (Vol. 879, pp. 714-719). Trans Tech Publications Ltd.

[14] Anchev, A.; Kaisheva, D.; Kotlarski, G.; Dunchev, V.; Stoyanov, B.; Ormanova, M.; Atanasova, M.; Todorov, V.; Daskalova, P.; Valkov, S. Welding of Ti6Al4V and Al6082-T6 Alloys by a Scanning Electron Beam. *Metals* (2023), 13, 1252.

[15] Kar J., Roy S.K., Roy G.G. Effect of beam oscillation on electron beam welding of copper with AISI-304 stainless steel. *J. Mater. Process. Tech.* 233 (2016) 174–185

[16] Hussain, M. Z., Xiong, J. T., Li, J., Siddique, F., Zhang, L. J., & Zhou, X. R. (2021). A study on strengthening and toughening mechanism of laser beam welded joint prepared between Ti–22Al–27Nb and Ti–6Al–4V with an interlayer of Nb. *Materials Science and Engineering: A*, *825*, 141843.